2012 10th International Conference on Frontiers of Information Technology

Adaptive NeuroFuzzy Wavelet Based SSSC Damping Control Paradigm

Rabiah Badar
Department of Electrical Engineering
COMSATS Institute of Information Technology
Abbottabad, Pakistan
Email: rabiahbadar@ciit.net.pk

Laiq Khan
Department of Electrical Engineering
COMSATS Institute of Information Technology
Abbottabad, Pakistan
Email: laiq@ciit.net.pk

***Abstract*—The supplementary damping control can be efficiently used for Flexible AC Transmission System (FACTS) controllers to damp the low frequency oscillations in single and multi-machine power systems. These low frequency oscillations may lead to the instability of the system if not damped out properly. This paper presents, wavelet based adaptive NeuroFuzzy supplementary control by incorporating wavelets in the structure of Conventional Adaptive Fuzzy NN (CAFNN) for SSSC. The proposed control system has successfully been applied to single machine infinite bus system (SMIB) and multi-machine power system for various faults and operating conditions. Finally, the proposed control technique is compared with CAFNN using nonlinear time domain simulations for various faults and operating conditions. The results reveal that the proposed control has optimal damping performance as compared to CAFNN for both local and inter-area modes of oscillation.**

***Keywords*-SSSC; adaptive NeuroFuzzy control; wavelets; SMIB; multi-machine power system**

I. Introduction

Low frequency oscillation, ranging from 0.2 to 3 Hz, is an inherent phenomenon in large interconnected power systems. The immediate solution to this problem is the installation of a power system stabilizer or some automatic voltage regulator [1]. But due to the simplicity, linearity and local control of these devices their installation is not much effective in multivariable, highly nonlinear power system. Therefore, efforts are being made to control these oscillations through transmission side as well which lead to the emergence of FACTS controllers. Static Synchronous Series Compensator (SSSC) is a power electronic based controller of FACTS family which has the proven ability of controlling the power flow on a line and stability enhancement as being widely used and discussed in literature [2-4]. The role of auxiliary stabilizing signal, the choice of the controller input signal, effect of mode of operation, degree of compensation and optimal location of SSSC has been discussed in [5-8].

SSSC can be used to damp power system oscillations using supplementary damping control. Most of the proposed control schemes for oscillations damping control like PID, eigenvalue assignment, pole placement, mathematical programming etc. are linear in nature and do not provide good control over wide range of operating conditions. On the other hand, the nonlinear control techniques have inherent mathematical and structural complexities. Moreover, due to highly time varying nature of power system the control must be able to adapt the changes in the system, almost instantaneously. In [9], Dash et al. used nonlinear TSK for damping power system oscillations using FACTS. They proposed that nonlinear function in consequent part of conventional TSK can significantly improve the controller performance. However, the performance of the proposed control has not been checked in terms of series of faults occurring in the system at different time instants. Moreover, conventional NeuroFuzzy structure with fixed parameters architecture cannot ensure the online training of the network and thus perform well only at a specific operating point.

This paper presents a wavelet based online adaptive NeuroFuzzy supplementary damping control (SDC) to improve the transient and steady-state stability of the power system by incorporating wavelet NNs in the consequent part of CAFNN. Different structures of Fuzzy wavelet NNs have been proposed in literature. They have vast application horizon due to their fast learning and control capability for nonlinear dynamic systems [10-12]. The wavelet NNs proposed so far in literature can mainly be divided into two types. One type of wavelet networks utilizes continuous wavelet basis in its hidden layer as activation functions while the other uses discrete.

In case of continuous wavelet function NNs both the dilation and translation parameters can be modified in addition to the weights of the output layer, whereas, in discrete wavelets NNs only weights of final layer can be modified. The control of both dilation and translation parameters, in case of continuous wavelet functions, causes the change in scale which can increase the computational burden in large dimensional problems. To evade this problem wavelet NNs were combined with fuzzy systems known as fuzzy wavelet NNs [13]. The main objective of this article is:

- to present an Adaptive NeuroFuzzy Wavelet Network (ANFWN) based SDC for SSSC to damp local and inter-area modes of oscillation.
- to compare the results of the proposed algorithm with

978-0-7695-4927-9/12 $26.00 © 2012 IEEE
DOI 10.1109/FIT.2012.27

those of a conventional TSK fuzzy controller.

- to study the performance of the two approaches for different operating conditions and disturbances.

The rest of the paper is arranged as follows; section II gives the mathematical model of power system installed with SSSC. The control system is designed in section III. The details of test systems and simulation results are presented and discussed in section IV and finally section V concludes the findings of this research.

II. Power System Installed with SSSC

SSSC is a series compensating FACTS controller which controls the power flow on a transmission line by injecting a controllable series voltage in quadrature with the line current. In this way, it emulates an inductive or capacitive reactance [8]. The controller can be made to operate in either mode of operation by varying the magnitude and phase of the injected voltage. During post-fault conditions the injected reference voltage deviates from its reference value, therefore, an auxiliary damping signal is introduced to adjust the bus voltage magnitude at its reference value. That is, the control must drive the SSSC modulation index m and the phase angle ϕ to the desired value in order to regulate the injected voltage of the series converter, via internal control.
Let $I\angle\theta$ be the current flowing through line then the converter output voltage in phasor form is given by,

$$\overline{V}_{conv} = mkV_{DC}\angle\psi_s \tag{1}$$

Where, $\psi_s = \theta + \phi$. Here, ϕ is the firing angle, m is the modulation index and k is a constant defining the relationship between converter AC and DC side voltages [5]. The DC side voltage can be calculated by law of power conservation and is given as;

$$\frac{dV_{DC}}{dt} = \frac{3mk}{2C}[i_d\cos\psi_s + i_q\sin\psi_s] - \frac{V_{DC}}{CR_{DC}} \tag{2}$$

Fig. 1 shows SSSC installed on a line between nodes i and j and its supplementary damping control setup. Let $\overline{V}_1$ and $\overline{V}_2$ be the sending and receiving end voltages, respectively. In case of SMIB test system, $\overline{V}_1$ and $\overline{V}_2$ are the machine and infinite bus voltages, respectively.

The generator terminal voltage in phasor form is given by,

$$\overline{V}_{tg} = j\overline{I}_{x_\Sigma} + \overline{V}_{conv} + \overline{V}_2 \tag{3}$$

Where, x_Σ is the total reactance of the system including the line reactance and SSSC. Using (1), (3) and sixth-order generator model with q-axis leading d-axis the generator current, in dq components, can be written as;

$$I_d = (E''_q - V_2\cos\delta - mkV_{DC}\sin\psi_s)/(x_\Sigma + x''_d) \tag{4}$$

$$I_q = (V_2\sin\delta - mkV_{DC}\cos\psi_s)/(x_\Sigma + x''_q) \tag{5}$$

In case of multi-machine system, the generator current, in network coordinates, can be written in the following form by

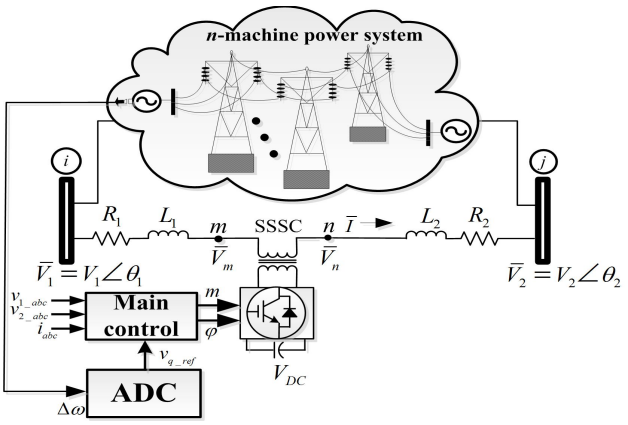

Figure 1: Power system with SSSC

solving for the admittance matrix of power system reduced at generator nodes and installed with SSSC.

$$\overline{\boldsymbol{I}}_g = \overline{\boldsymbol{C}}_Y\overline{\boldsymbol{V}}_{tg} + \overline{\boldsymbol{C}}_o\overline{V}_{conv} \tag{6}$$

Where,

$$\overline{\boldsymbol{C}}_Y = \left(\overline{\boldsymbol{Y}}_{gg} - \begin{bmatrix}\overline{\boldsymbol{Y}}_{g1} & \overline{\boldsymbol{Y}}_{g2}\end{bmatrix}\overline{\boldsymbol{Y}}^{-1}_{\vartheta_{12}}\begin{bmatrix}\overline{\boldsymbol{Y}}_{g1}\\ \overline{\boldsymbol{Y}}_{g2}\end{bmatrix}\right)$$

$$\overline{\boldsymbol{C}}_o = \begin{bmatrix}\overline{\boldsymbol{Y}}_{g1} & \overline{\boldsymbol{Y}}_{g2}\end{bmatrix}\overline{\boldsymbol{Y}}^{-1}_{\vartheta_{12}}\begin{bmatrix}\frac{1}{jx_\Sigma}\\ -\frac{1}{jx_\Sigma}\end{bmatrix}$$

and

$$\overline{\boldsymbol{Y}}^{-1}_{\vartheta_{12}} = \begin{bmatrix}\overline{Y}'_{11} + \frac{1}{jx_\Sigma} & -\frac{1}{jx_\Sigma}\\ -\frac{1}{jx_\Sigma} & \overline{Y}'_{22} + \frac{1}{jx_\Sigma}\end{bmatrix}$$

Where, $\overline{Y}'_{11}$ and $\overline{Y}'_{22}$ are the admittances after the installation of SSSC.

III. ANFWN based control system design

Fig. 2 shows the closed-loop structure of the system. Here, $\Xi_\tau \in \{d_{s\_dis} \cup d_{l\_dis}\}$ is the disturbance applied to the system, represents the set of small disturbances and is the set of large disturbances. $\tau = 1, 2, , p$, where, p is the total number of disturbances. The proposed control scheme is model free direct adaptive control based on controller output matching method. The relative output error and its derivative are taken as inputs to the control block. Plant includes the power system along with SSSC and its internal control. The proposed ANFWN is a modified version of the conventional TSK structure by incorporating the wavelets in the consequent part. The Morelet wavelet function is chosen for this purpose and is given by,

$$\varphi_j(x_i) = \cos(5q_j)e^{-\frac{q_j^2}{2}} \tag{7}$$

Where, $q_j = \frac{x_i - b_j}{a_j}$. Here, a_j and b_j are the dilation and translation factors of the wavelet, respectively, and is the

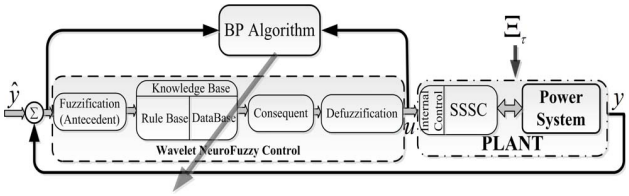

Figure 2: Closed-loop system structure

ith input to the network. Morelet wavelet function is a non-orthogonal function of Gaussian probability density function and cosine function with most of the energy concentrated in the vicinity of origin.

The antecedent part uses Gaussian membership function to describe the input linguistic variable. $T-norm$ product operator is used to calculate the strength of each rule. The Gaussian membership function for ith input and jth rule is given by,

$$\wp_j(x_i) = e^{-\frac{(x_i-h_{ij})^2}{\varsigma_{ij}^2}} \tag{8}$$

The proposed multiple-input-single-output (MISO) network architecture is based on IF THEN rules of the following generalized form,

$$R_j: If\ x_{1j}\ is\ \wp_{1j}\ and\ x_{2j}\ is\ \wp_{2j}\cdots x_{mj}\ is\ \wp_{mj}\ then\ y_j = \zeta_j$$

Here, R_j denotes the jth fuzzy rule, x_{ij} is the ith input to the jth fuzzy rule, such that $i = 1,\ 2,\ \cdots,\ m$ with m being the total number of inputs.

$$\mu_j = T[\wp_1\ \wp_2\ \wp_3\ \cdots\ \wp_n] \tag{9}$$

Where, μ_j is the firing strength of jth rule and n is the number of membership functions in a rule.

The final output of the network is given by,

$$u = \frac{\sum_{i=1}^{n}\mu_i\zeta_i}{\sum_{i=1}^{n}\mu_i} = \Im\Psi \tag{10}$$

Where, $\Im = [\Im_1\ \Im_2\ \Im_3\ \cdots\ \Im_n]$ and $\Im_i = \frac{\mu_i}{\sum_{i=1}^{n}\mu_i}$ known as fuzzy basis functions (FBFn). $\Psi = [\zeta_1\ \zeta_2\ \zeta_3\ \cdots\ \zeta_n]$ is the output of the wavelet network. The wavelet network consists of three layers; the input layer, hidden wavelet layer and the output layer. The κth output of the network is given as,

$$\zeta_\kappa = w_\kappa \sum_{i=1}^{m}\varphi_\kappa(x_i) \tag{11}$$

Where, w_κ's are the weights of the output layer.

The overall network architecture is shown in Fig. 3 and can mainly be divided in two parts i.e. the antecedent and the consequent part. Antecedent part includes layer 1, layer 2 and layer 3, whereas, the consequent part consists of layer 4-layer 6.

Layer 1 is the input layer which takes the input and passes it to layer 2. The input vector is fuzzified in layer 2 using (8)

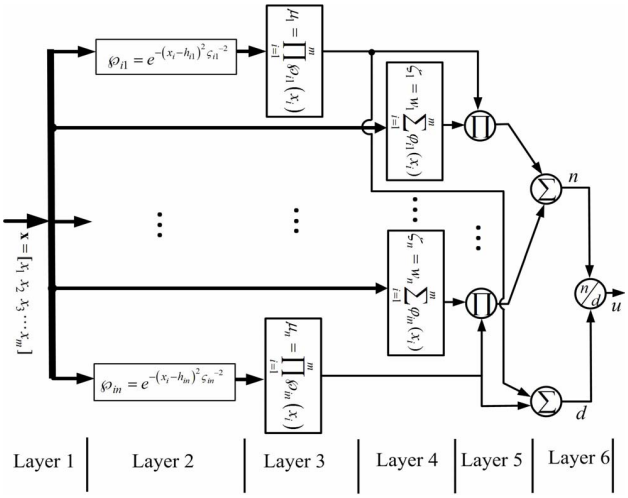

Figure 3: Adaptive NeuroFuzzy wavelet architecture

and the strength of each rule is computed using (9) in layer 3. Layer 4 is the consequent layer which contains wavelet NNs in each processing node and basically works in parallel with layer 2. The output of this layer is calculated using (11). Layer 5 is the product layer which multiplies the outputs of layer 2 and layer 4. Finally, the defuzzification is carried out in layer 6 using (10).

A. Parameters Update Algorithm

Gradient descent based back-propagation learning algorithm is used for parameters adaptation, by minimizing the following cost function;

$$E = \frac{1}{2}(\hat{y}-y)^2 + \frac{\hbar}{2}u^2 \tag{12}$$

Where, $\hat{y}$ and y are the desired and actual outputs of the plant, respectively. 'u' is the control output. The cost function is used to get optimal results for control performance with minimum control effort. The parameters update law is given as;

$$\Phi(t+1) = \Phi(t) + \Delta\Phi(t) + \lambda(\Phi(t) - \Phi(t-1)) \tag{13}$$

Where, $\Delta\Phi(t) = -\eta\frac{\partial E}{\partial\Phi}$, $\Phi = [h_{ij}\ \varsigma_{ij}\ a_{ij}\ b_{ij}\ w_{ij}]$ is the adaptation parameters vector and η is the learning rate. λ is the momentum term which guarantees the stability of the algorithm and speeds up the convergence.

The differential is simplified by using the following chain rule of calculus.

$$\frac{\partial E}{\partial\Phi} = \left(\frac{\partial E}{\partial y}\frac{\partial y}{\partial u} + \hbar u\right)\frac{\partial u}{\partial\Phi} \tag{14}$$

Such that $\frac{\partial e}{\partial y} = -e$, where, $e = \hat{y} - y$ is the error input to the control system such that $\hat{y}$ and y represent the desired and actual outputs of the plant, respectively. The configuration shown in Fig. 2 is based on direct adaptation

method to eliminate the need of plant model. Using direct output matching method it can be assumed that $\frac{\partial y}{\partial u} = 1$ [14]. Therefore, the parameters can be updated using the following chain rules;

$$\frac{\partial E}{\partial h_{ij}} = \sum_j e_c \frac{\partial u}{\partial \mu_j} \frac{\partial \mu_j}{\partial \wp_{ij}} \frac{\partial \wp_{ij}}{\partial h_{ij}} \quad (15)$$

$$\frac{\partial E}{\partial \varsigma_{ij}} = \sum_j e_c \frac{\partial u}{\partial \mu_j} \frac{\partial \mu_j}{\partial \wp_{ij}} \frac{\partial \wp_{ij}}{\partial \varsigma_{ij}} \quad (16)$$

$$\frac{\partial E}{\partial a_{i\kappa}} = e_c \frac{\partial u}{\partial \zeta_j} \frac{\partial \zeta_j}{\partial q_{ij}} \frac{\partial q_{ij}}{\partial a_{i\kappa}} \quad (17)$$

$$\frac{\partial E}{\partial b_{i\kappa}} = e_c \frac{\partial u}{\partial \zeta_j} \frac{\partial \zeta_j}{\partial q_{ij}} \frac{\partial q_{ij}}{\partial b_{i\kappa}} \quad (18)$$

$$\frac{\partial E}{\partial w_{i\kappa}} = e_c \frac{\partial u}{\partial \zeta_j} \frac{\partial \zeta_j}{\partial w_{i\kappa}} \quad (19)$$

Where, $e_c = -\left(e\frac{\partial y}{\partial u} - \hbar u\right)$.

$$\frac{\partial E}{\partial h_{ij}} = \sum_j e_c(t) \frac{y_j - u}{\sum_j \mu_j} \mu_j(x_i) \frac{2(x_i - h_{ij})}{\varsigma_{ij}^2} \quad (20)$$

$$\frac{\partial E}{\partial \varsigma_{ij}} = \sum_j e_c(t) \frac{y_j - u}{\sum_j \mu_j} \mu_j(x_i) \frac{2(x_i - h_{ij})^2}{\varsigma_{ij}^3} \quad (21)$$

$$\frac{\partial E}{\partial a_{i\kappa}} = \rho_\kappa q_{i\kappa} \left(\frac{\varphi_{i\kappa} q_{i\kappa} + 5e^{-0.5q_{i\kappa}^2} \sin(5q_{i\kappa})}{a_{i\kappa}} \right) \quad (22)$$

$$\frac{\partial E}{\partial b_{i\kappa}} = \rho_\kappa \left(\frac{\varphi_{i\kappa} q_{i\kappa} + 5e^{-0.5q_{i\kappa}^2} \sin(5q_{i\kappa})}{a_{i\kappa}} \right) \quad (23)$$

$$\frac{\partial E}{\partial w_{i\kappa}} = e_c(t) \mu_\kappa(x_i) \varphi(q_{ik}) \left[\sum_{\kappa=1}^{n} \mu_\kappa(x_i) \right]^{-1} \quad (24)$$

Where, $\rho_\kappa = e_c \mu_\kappa w_\kappa / \sum_{\kappa=1}^{n} \mu_\kappa$.
The final update equations can be found using (12). The update parameters are initialized randomly in the interval [0 1]. The learning rate of the ANFWN is adjusted adaptively following the trend in relative error deviation. If the error deviation is negative the value of learning rate is decreased, whereas, increased in case of positive error deviation, to guarantee the stability of the system [12].

IV. Simulation Results and Discussion

In order to validate the performance of the proposed network for local and inter-area modes of oscillation, SMIB and a four-machine, two-area power system is considered. The simulations are carried out at 100 MVA base. The number of inputs to the fuzzy control system and membership functions for each input is two. The speed deviation and derivative of the speed deviation are taken as two inputs to the controller. The number of parameters to be updated, for antecedent and consequent parts, is 10 and 18 for CAFNN and ANFWN, respectively. The details of each system and simulation results are as follows;

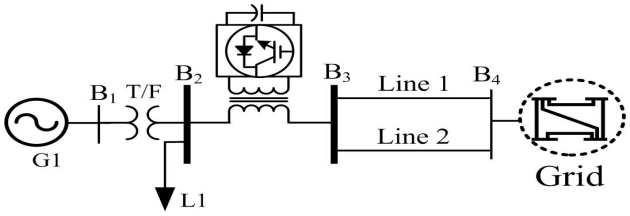

Figure 4: SMIB test system

A. Case-I: SMIB Nominal Loading

SMIB test system is considered basically to validate the performance of the proposed controller for local mode of oscillation. The test system used for simulations is shown in Fig. 4. The detail of system parameters can be found in [15]. The operating condition for nominal loading is $P_0 = 0.75 p.u.$ and $\delta_0 = 20.2^0$. A three cycles, 3-φ, self-clearing fault is applied at the middle of one of the lines connecting buses B3 and B4, at t=0.5 s. This severe fault remains on the system for 0.05 s and then restores the system to its original condition. The performance comparison of both control techniques for this type of fault is shown in Fig. 5. The plots in Figs. 5(a)-(c) are the speed deviation ($\Delta\omega$); load angle (δ) and real power flow on transmission line, measured at bus B4 (P_L). It is clear from these results that ANFWN control has good performance as compared to no control and CAFNN cases in terms of settling time and overshoot.

B. Case-II: SMIB Heavy Loading

The robustness of the controller is further verified by changing the loading condition from nominal to heavy loading. The operating condition for this case is $P_0 = 1$ p.u. and $\delta_0 = 24.74^0$. The applied fault type and duration is same as discussed for the case of nominal loading. In this case, application of this severe fault causes the system to lose synchronism. The simulation results for this contingency are shown in Figs. 6(a)-(c). It can be seen from these figures that ANFWN has better damping performance as compared to CAFNN.

C. Case-III: Multimachine Test System under Series of Faults

To check the robustness of proposed control system in more practical scenario and stressed condition, a four-machine, two-area system is considered. The system model is shown in Fig. 7. Generators G1 and G2 are in area 1, whereas, generators G3 and G4 are in area 2. The simulations are carried out taking G2 as swing bus and the other three generators as PV generator buses. Each generator is equipped with hydraulic turbine system and DC type 1 excitation system. The PSS on each exciter are disabled and the whole damping is provided through SSSC, installed at the middle of the power system. The parameters detail of the

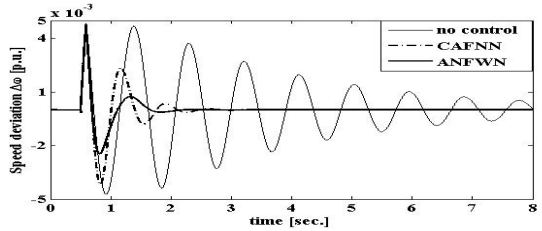

(a)

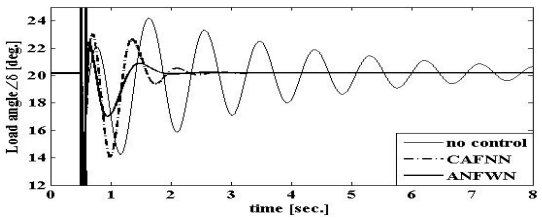

(b)

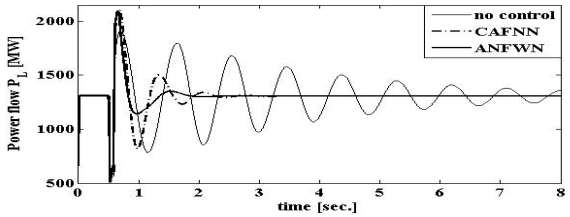

(c)

Figure 5: Case 1-SMIB nominal loading: (a) Rotor speed deviation, (b) Load angle, (c) Line power flow

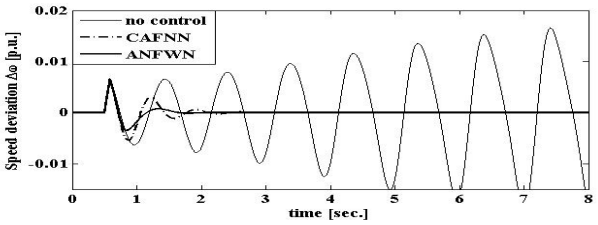

(a)

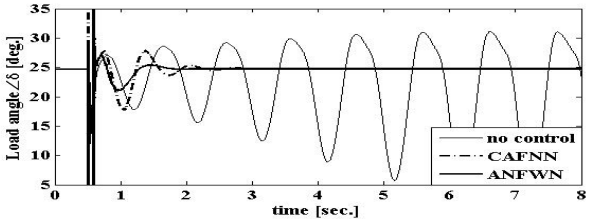

(b)

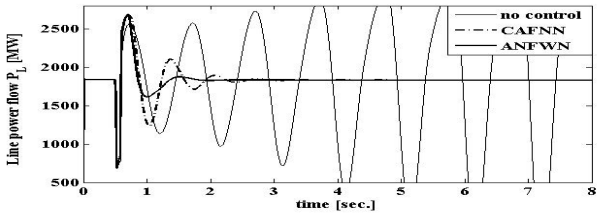

(c)

Figure 6: Case II-SMIB heavy loading: (a) Rotor speed deviation, (b) Load angle, (c) Line power flow

system can be found in [16]. The robustness of ANFWN for change in fault location and operating condition is tested by applying a series of faults. A 3-φ fault of duration 8-cycles is applied on line 2, near area 1, at t=1 sec. The fault is cleared by opening the line at t=1.33 sec. The line is re-closed at t=7 sec. Fig. 8 shows the results for inter-area and local modes of oscillation for this contingency.

It is clear from Fig. 9 that application of SDC restores the system stability. ANFWN efficiently damps the oscillations for local and inter-area modes. The simulation results show that CAFNN being adaptive and intelligent has competent results. Therefore, different performance indices are used to analyze the performance more clearly in transient and steady-state regions. The performance index is the integral of a function of time and error function of the system parameter. It can be written generally as,

$$\text{Performance Index, } PI = \int_0^{t_s} f(t, e(t))dt \qquad (25)$$

Where, t_s is the simulation time and $f(t, e(t)) = t^p \left(\sum_{i=1}^{n} (\mid \Delta\omega_{L_i} \mid^q + \mid \Delta\omega_{L_i} \mid^p)\right)$. L and I represent the local and inter-area modes of oscillation, respectively. i is the mode number, p and q are fixed numbers, such that for IAE, ISE, ITAE and ITSE, respectively. The second term in $f(t, e(t))$ vanishes in case of SMIB test system.

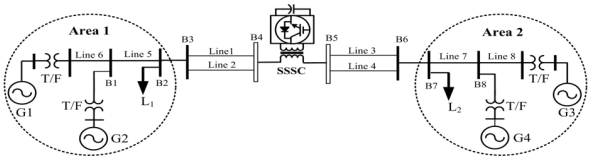

Figure 7: Multi-machine test system

The corresponding results for performance improvement are given in Table I. The statistics presented in Table 1 show that the overall percent improvement in case of SMIB heavy loading and series fault of multi-machine is greater than improvement in case of SMIB nominal loading and 3-φ fault of multi-machine test system, respectively, which shows that CAFNN can perform well in relatively simple situations and when the system is under more stressed condition then its performance degrades.

Table I: Performance improvement for ANFWN (%)

Performance Index	Case-I	Case-II	Case-III
ITAE	45.58	50.48	8.72
ITSE	58.25	53.41	11.07
IAE	39.32	39.85	8.33
ISE	52.35	45.39	9.25

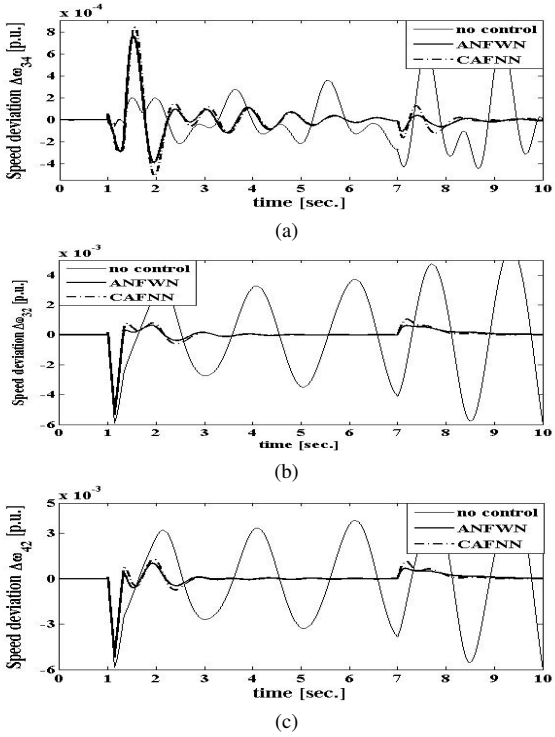

Figure 8: Case III-Multi-machine test system: (a) Local mode; (b) and (c) Inter-area modes of oscillation

V. Conclusion

In this paper, a wavelet based NeuroFuzzy control system has been proposed as supplementary damping control of SSSC and applied to different power systems for damping low frequency oscillations. Gradient descent technique is used to optimize the control parameters in order to maintain the computational simplicity and speed of the proposed control system, other optimization techniques can be used for performance improvement but at the cost of complexity. The performance of the proposed control system is optimal for both local and inter-area modes of oscillation. It can be concluded that only SSSC without any supplementary control fails to maintain the system stability in most of the test cases. The simulations further reveal that the application of ANFWN supplementary control finally eliminates the need of PSS on each machine in a multi- machine power system, which makes the system cost-effective, as well.

References

[1] B. Singh, N. K. Sharma, A. N. Tiwari, K. S. Verma, and D. Singh, "A status review of incorporation of FACTS controllers in multimachine power systems for enhancement of damping of power system and voltage stability," *Intr. Jr. Engg. Sci. Tech.*, vol. 2, no. 6, pp. 1507-1525, 2010.

[2] X. P. Zhang, "dvanced modeling of the multicontrol functional static synchronous series compensator (SSSC) in Newton power flow," *IEEE Trans. Power Syst.*, vol. 18, no. 4, pp. 1410-1416, 2003.

[3] S. K. Saha, "Reliability contingency analysis by static synchronouus series compensator in optimal power flow," *Intr. Jr. Comp. Electr. Engg.*,vol. 2, no. 5, pp. 908-911, 2010.

[4] H. N. Aghdam, "Analysis of static synchronous series compensators (SSSC) on congestion managment and voltage profile in power system by PSAT toolbox," *Research Jr. App. Sci., Engg. Tech.*, vol. 3, no. 7, pp. 660-667, 2011.

[5] H. F. Wang, "Static synchronous series compensator to damp power system oscillations," *Electric Power Systems Research*, vol. 54, no. 2, pp. 113-119, 2000.

[6] I. Ngamroo, J. Tippayachai and S. Dechanupapittha, "Robust decentralised frequency stabilisers design of static synchronous series compensators by taking system uncertainties into consideration," *Inter. Jr. Elect. Power Energy Syst.*, vol. 28, no. 8, pp. 513-524, 2006.

[7] F. A. R. Al-Jowder, "Influence of mode of operation of the SSSC on the small disturbance and transient stability of a radial power system," *IEEE Trans. on Power Syst.*, vol. 20, no. 2, pp. 935-942, 2005.

[8] S. Panda, S. C. Swain, P. K. Rautray, R. K. Malik, and G. Panda, "Design and analysis of SSSC-based suplementary damping controller," *Sim. Model. Prac. Theory,* vol. 18, no. 9, pp. 1199-1213, 2010.

[9] P. K. Dash and S. Mishra, "Damping of multimodal power system oscillations by FACTS devices using nonlinear Takagi-Sugeno fuzzy controller," *Electr. Power Energy Syst.*, vol. 25, no. 6, pp. 481-490, 2003.

[10] M. Zekri, S. Sadri, and F. Sheikholeslam, "Adaptive fuzzy wavelet network control design for nonlinear systems," *Fuzzy Sets and Systems,* vol. 159, no. 20, pp. 2668-2695, 2008.

[11] L. Chi-Huang, "Wavelet fuzzy neural networks for identification and predictive control of dynamic systems," *IEEE Trans. on Indust. Electr.*, vol. 58, no. 7, pp. 3046-3058, 2011.

[12] R. H. Abiyev, and O. Kaynak, "Fuzzy wavelet neural networks for identification and control of dynamic plants-A novel structure and comparative study," *IEEE Trans. on Industrial Electronics*, vol. 55, no. 8, pp. 3133-3140, 2008.

[13] A. Ebadat, N. Noroozi, A. A. Safavi, and S. H. Mousavi, "Modeling and control of nonlinear systems using novel fuzzy wavelet networks: The modeling approach," In *Proc. 49th IEEE Conf. on Decision and Control*, Atlanta, USA, pp. 3475-3480, 2010.

[14] Z. Liu, "Self-tuning control of electrical machines using gradient descent optimization," *Optimal Control Applications and Methods*, vol. 28, no. 2, pp. 77-93, 2006.

[15] S. Panda, N. P. Padhy, and R. N. Patel, "Power system stability improvement by PSO optimized SSSC-based damping controller,"*Electric Power Components and Systems*, vol. 36, no. 5, pp. 468-490, 2008.

[16] P. Kundur, *Power System Stability and Control* (McGraw-Hill, NY: 1994).